Investigation of the adsorption mechanism of heterocyclic molecules on copper using potentiodynamic ORP-EIS and in-situ Raman spectroscopy

Reference:

Geboes Bart, Baert Kitty, Hubin Annick, Breugelmans Tom.- *Investigation of the adsorption mechanism of heterocyclic molecules on copper using potentiodynamic ORP-EIS and in-situ Raman spectroscopy*

Electrochimica acta - ISSN 0013-4686 - (2015), p. 1-22

DOI: http://dx.doi.org/doi:10.1016/j.electacta.2015.01.036

Handle: http://hdl.handle.net/10067/1223520151162165141

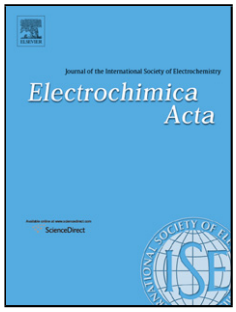

Title: Investigation of the Adsorption Mechanism of HeterocyclicMolecules on Copper using Potentiodynamic ORP-EIS and In-situ Ramanspectroscopy

Author: Bart Geboes Kitty Baert Annick Hubin Tom Breugelmans

PII: S0013-4686(15)00056-0
DOI: http://dx.doi.org/doi:10.1016/j.electacta.2015.01.036
Reference: EA 24088

To appear in: *Electrochimica Acta*

Received date: 13-10-2014
Revised date: 31-12-2014
Accepted date: 9-1-2015

Please cite this article as: Bart Geboes, Kitty Baert, Annick Hubin, Tom Breugelmans, Investigation of the Adsorption Mechanism of HeterocyclicMolecules on Copper using Potentiodynamic ORP-EIS and In-situ Ramanspectroscopy, *Electrochimica Acta* (2015), http://dx.doi.org/10.1016/j.electacta.2015.01.036

Investigation of the Adsorption Mechanism of Heterocyclic Molecules on Copper using Potentiodynamic ORP-EIS and In-situ Raman spectroscopy

Bart Geboes[a,b], Kitty Baert[a], Annick Hubin[a], Tom Breugelmans[a,b,*]

[a] *Vrije Universiteit Brussel, Research Group Electrochemical and Surface Engineering, Pleinlaan 2, 1050 Brussels, Belgium*
[b] *University of Antwerp, Research Group Advanced Reactor Technology, Salesianenlaan 90, 2660 Hoboken, Belgium*

Abstract

The adsorption mechanism of 2-amino-5-mercapto-1,3,4-thiadiazole (AMTD) and 2-methyl-5-mercapto-1,3,4-thiadiazole (MMTD) was investigated by a combined electrochemical and surface analysis approach. The link with the adsorption kinetics was maintained during AC voltammetry as well as during potentiodynamic broadband multisine (ORP-EIS) measurements. A discrepancy between the thickness of the adsorbate layers determined by both techniques was identified as a result of the frequency dispersion of the system. The use of a broad frequency range and the statistical evaluation with ORP-EIS deemed this the preferential technique for layer thickness determination. The surface-molecular complex was further investigated through in-situ surface enhanced Raman spectroscopy (SERS), collected under identical electrochemical conditions. The adsorption regions defined by the AC voltammetry measurements corresponded to the SERS response. The proposed adsorption orientation for AMTD and MMTD was through N^4-S-Cu σ-bonding. A layer thickness of 0.76 nm and 0.85 nm respectively indicated the formation of multiple adsorbed

*Corresponding author
Email addresses: bart.geboes@uantwerpen.be (Bart Geboes), kibaert@vub.ac.be (Kitty Baert), anhubin@vub.ac.be (Annick Hubin), tom.breugelmans@uantwerpen.be (Tom Breugelmans)

molecular layers. Application of the in-situ approach on small heterocyclic molecules derived from AMTD and MMTD indicated the importance of adjacent nitrogen atoms in a five membered heterocyclic ring for the adsorbate-substrate complex.

Keywords:
Adsorption mechanism, Heterocycles, Mercaptothiadiazole, In-situ SERS, Potentiodynamic ORP-EIS

1. Introduction

Adsorption of organic substances on metal substrates represents an active research direction. This is due to the recognition of both the practical and the scientific importance of surface modification. From one side, the creation of functionalised substrates is important for a variety of applications in the fields of biotechnology [1, 2], organic based electronics [3], and surface protection [4]. From the other, deposition of ultra thin organic monolayers serves as a scientific platform for fundamental investigation of various interface related phenomena [5, 6].

Both 2-amino-5-mercapto-1,3,4-thiadiazole (AMTD) and 2-methyl-5-mercapto-1,3,4-thiadiazole (MMTD) are corrosion inhibitors derived from the toxic 2-mercaptobenzothiazole (MBT) [7, 8]. The mercapto group in both molecules is expected to interact with the metal surface in a similar way as the widely investigated alkane thiols [9]. AMTD and MMTD are both nitrogen-sulphur mixed donor ligands and thus differ significantly from alkane thiols as they can react with the substrate by a number of alternative coordination modes.

Over the course of our previous work the adsorption process of heterocyclic molecules was studied intensively with a variety of electrochemical techniques. Electrochemical impedance spectroscopy (EIS) was performed on AMTD and MMTD in neutral chloride solutions and an electrical equivalent circuit (EEC)

was proposed, supported by quantum chemical investigations [4]. A characteristic feature of this EEC is the presence of interfacial phases between the bulk metal and the oxide and between the bulk oxide and the electrolyte. These results where incorporated in a study of AMTD, MMTD and a selection of small heterocyclic molecules using a broadband multisine excitation signal for EIS [10]. These experiments were done in floating mode and not at a potentiostat locked OCP value. Thus, the application of trend compensating currents because of a change in the system state during the experiment was prevented. A strong influence of the molecular conformation on the electrochemical response could be detected under these circumstances. Later on our group studied the adsorption mechanism of MMTD in more detail by determining the influence of potential and polarisation conditions on the adsorption kinetics [11]. Potentiodynamic EIS proved to be a powerful technique for investigating the adsorption process of heterocycles because a link with the kinetics is maintained in contrast to conventional EIS. Additionally a more accurate estimate of the capacitance of adsorbed molecular layers was achieved compared to differential capacitance measurements as a result of the broader frequency range and statistical evaluation of measurement data.

By measuring the capacitance values of organic layers, information on reorientation and adsorption-desorption of the organic molecules is provided. However, no direct conclusions can be made about layer thickness and orientation modes of the adsorbed molecules that cause these capacitance values. In order to transform the capacitance into layer thickness and orientation mode, additional information on the molecular dimensions and properties is needed. Complementary surface analysis techniques such as spectroscopic ellipsometry (SE), FTIR or Raman spectroscopy are thus inevitable in electrochemical studies towards adsorption phenomena. Because of its ability to provide direct molecular information from vibrational spectra in-situ, Raman spectroscopy is widely applied for the investigation of adsorption processes on different metals [12, 13] and has already been used successfully in conjunction with differential capacitance mea-

surements [14–16]. In view of the weak Raman signal, an enhancement (SERS) by use of colloidal aggregates or roughened surfaces is usually sought [17–19]. The method allows to obtain qualitative information relatively easy if the organic compound is adsorbed or desorbed.

Therefore the scope of this work is to further elucidate the adsorption mechanism and geometry of the surface- molecular complex of AMTD and MMTD using a combined electrochemical and surface analysis approach. The application of Potentiodynamic Odd Random Phase Electrochemical Impedance Spectroscopy (PD ORP-EIS) in combination with in-situ SERS measurements is performed. The fast acquisition of a full range of frequencies with ORP-EIS makes this recently developed technique suitable for potentiodynamic impedance measurements. In addition to the short measurement time, also essential statistical information concerning the noise level, linear and stationary behaviour is provided during the potentiodynamic scan [20]. Besides AMTD and MMTD some small heterocyclic molecules (triazole, imidazole, pyrazine and pyridazine) are also investigated in this work. The compounds are chosen in a way allowing to systematically study the influence of the heteroatom position and number. Such a study is important because the knowledge of the alteration brought by the chemical bonding can facilitate the guided development of application tuned adsorption systems. This approach maintains the link with adsorption kinetics and provides a better understanding of the adsorption process of thin organic coatings. Insight in the formation of these thin organic coatings can enable progress in several important fields such as corrosion inhibition, organic based electronics and lithography.

2. Experimental

2.1. Compounds

Ultra-pure water (Milli-Q; 18.2 MΩ cm) is employed for all purposes including rinsing of the glassware. The copper electrochemical behaviour is in-

vestigated in a 0.1M NaF aqueous solution. NaF is used as a supporting electrolyte because of the low specific adsorption of the fluorine ion. All heterocyclic molecules under investigation (AMTD, MMTD, triazole, imidazole, pyrazine and pyridazine) are pro analysis grade from Merck® or Fluka® and are used as received to prepare 5 mM solutions.

2.2. Electrochemical characterisation

All the electrochemical experiments are carried out on a home-built set-up which consists of data aquisition (DAQ) cards, a waveform generator, a lock-in amplifier and a Bank Wenking Elektronik POS 2 potentiostat. A National Instruments 6024E DAQ-card is driven by a Labview vi algorithm and is exploited to carry out the AC voltammetry measurements. To obtain the differential capacitance curves, an analogue waveform generator is used to generate the low amplitude ac current (22 Hz) on top of the 2 mV/s potential sweep and a Signal Recovery 5105 lock-in-amplifier is used to determine the real and imaginary part of the measured current response. A National Instruments PCI-4461 DAQ-card with a built-in anti-aliasing filter performs the data generation and treatment of the PD ORP-EIS measurements. The multisine signal is simultaneously applied with a 2 mV/s potential sweep and is composed in the same manner as described earlier [21, 22].

The electrochemical cell configuration consists of a saturated calomel reference electrode (SCE) (all potentials in this work are reported against SCE), a platinum foil as counter electrode and a copper working electrode. This working electrode is a 99,9% pure copper rod with a diameter of 8 mm and embedded in an insulating polyvinylidene fluoride (PVDF) coating. To assure reproducible measurements, all electrodes are mechanically polished with the same procedure: diamond pastes with grain sizes of 320 µm, 9 µm, 3 µm and 0.04 µm are used respectively. Immediately before their use, the specimens are ultrasonically cleaned in methanol and chloroform (3 minutes each) and rinsed with water. After the rinsing, the samples are protected by a water cap and put in an electrochemical cell within 30 seconds.

The solution is preliminary purged (for 20 minutes) with nitrogen and the stream is kept through it for another 20 minutes. The nitrogen flow is redirected to form a protective blanket above the electrolyte during the measurement.

2.3. In-situ SERS measurements

Raman and SERS spectra are recorded by a Dilor XY Raman spectrometer in backscattering geometry. The spectrometer was coupled with an Olympus microscope, using 50x and 100x objectives. A Coherent Innova 70C Argon-Krypton mixed gas laser was employed to excitate 514 nm and 647 nm wavelengths. After filtering the Rayleigh scattered light with a notch filter, detection of scattered frequencies was done by means of a nitrogen cooled CCD detector. The EG&G PARC detector contains a diode array of 1024x256 pixels and a quantum efficiency of approximately 1 count per 10 photons. The energy resolution was over 2 cm^{-1}.

In order to obtain SERS measurements under polarization control a custom made cell is used, specially designed for combined electrochemical and SERS analysis. The spectrochemical cell is made of PVC and has 200 ml content. The SERS-active electrode is introduced face up on the bottom of the cell. A Ag/AgCl reference electrode and Pt foil counter electrode are used. The path of the incident and scattered light in the electrolyte solution is approximately 0.5 cm. The potential of the copper electrode is controlled by an Autolab PGSTAT10 potentiostat. The potential is swept with a scan rate of 2 mV/s between -1.16 V and 0.07 V vs. Ag/AgCl, which is identical to the conditions of the differential capacitance and potentiodynamic measurements. However, because of the minimum time needed to acquire a SERS spectrum, the step potential of the CV measurements is altered. Since it requires 60 seconds to measure a SERS spectrum in the spectral region of 900-1600 cm^{-1}, potential steps of 0.18 V are used.

Pretreatment of the working electrode to obtain a SERS active surface is done by galvanostatic roughening [23]. Copper electrodes are polished with grain size 1200 SiC grinding paper before galvanostatic pretreatment. The electrode

is immersed in a 0.2 M $CuSO_4$ and 0.4 M H_2SO_4 aqueous solution. A constant current of 75 mA/cm^2 is applied during 90 seconds.

3. Results and discussion

3.1. Electrochemical characterisation

3.1.1. Differential capacitance

The differential capacitance curve of the blank solution is shown in Figure 1 (red dashed line) as a reference for the capacitance of the investigated heterocyclic molecules. When no organic molecules are present the capacitance of the organic layer (C_{org}) is zero, and the measured total capacitance (C_T) will equal the double layer capacitance (C_{dl}) according to equation 1. Thus the shape of the plotted differential capacitance curve of the blank solution is a result of electrolyte species reorienting and migrating in the double layer under the influence of the varying electrode potential. Elucidating the mechanism of this double layer reorientation is not in the scope of this work and will not be further discussed. The lowest capacitance value of 22 μF cm^{-2} around -1 V can however serve as a reference for capacitance values of the heterocyclic adsorbate layers. This value also approximates the 16 μF cm^{-2} that is predicted by the Graham double layer model [24], considering the surface roughness of the copper electrodes used. Organic molecules that show similar values achieve little surface coverage and their contribution to the total measured capacitance is therefore limited.

$$C_T = (1 - \theta)\, C_{dl} + \theta\, C_{org} \tag{1}$$

The differential capacity curves obtained from AC voltammetry in Figure 1 (a) of pyrazine (dotted green line) and pyridazine (solid black line) exhibit little potential variation in the capacitance values. The increase in capacitance at low and high boundary potentials of the graph is most likely due to the hydrogen evolution and copper dissolution processes respectively, causing little surface coverage of the heterocycles. The decreasing capacitance in the region between

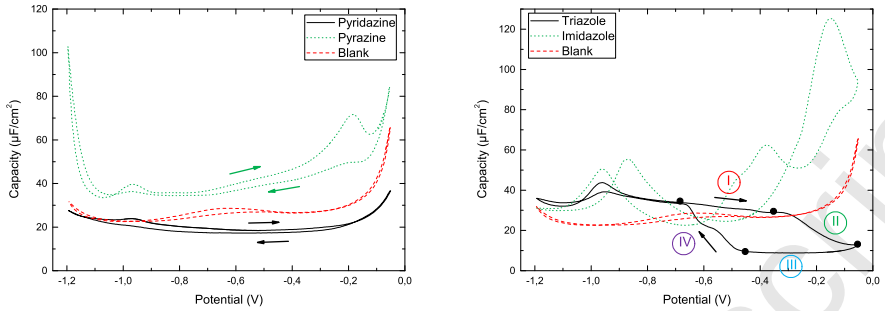

(a) (b)

Figure 1: Differential capacitance plots from AC voltammetry of a copper electrode in 0.1 M NaF + (a) 0.005 M Pyrazine-Pyridazine and (b) 0.005 M Triazole-Imidazole. All measurements are obtained after stabilisation through continuous cycling during 24 hours at 2 mV/s.

-0.2 V and -0.71 V in the cathodic scan of pyrazine could indicate a possible adsorption process. Hereafter, a constant capacitance is formed until -0.92 V. The increase in capacitance sets in at the opposite scan direction at -0.66 V. The adsorption plateau of pyrazine at 35 μF cm^{-2} is even higher compared to the value obtained in the blank solution (22 μF cm^{-2}). Calculating layer thickness is not apposite or possible for that matter, when this little surface coverage is achieved. Pyridazine shows a resembling differential capacitance curve. The major difference with pyrazine is the position of the constant capacity plateau, which amounts to 17 μF cm^{-2}.

When plotting the capacitance values for triazole and imidazole (Figure 1(b)) the outspoken difference in adsorption-desorption behaviour is underlined. It can be seen that imidazole (green dotted line) follows a complex curve. Compared to the blank there is no region with decreased capacitance which can indicate a specific adsorption of imidazole on the copper surface. Triazole (solid black line) on the other hand, has a significant lower capacitance (ca. 10 μF cm^{-2}) between -0.05 V and -0.5 V. The only structural difference between both molecules is the presence of adjacent nitrogen atoms in triazole. This feature appears to increase the adsorption strength, possibly by acting as an adsorption

center. This influence also holds for the relationship between pyrazine and pyridazine (adjacent nitrogen atoms are only present in pyridazine). The constant capacity plateau at 8.0 μF cm^{-2} corresponds to a layer thickness of 0.21 nm (ε_r = 2.2).

In the capacitance curve of triazole four regions can be differentiated, comparable to our earlier observations with MMTD [11]. Region I or the pre-adsorption stage (-0.69 V; -0.36 V) is suggested to result from a rearrangement of organic molecules in the electrode vicinity, prior to the adsorption process. The organic molecules in the double layer migrate to the electrode surface without interacting with it. In region II the electrochemical adsorption takes place. The sudden capacity decrease results from the growing layer thickness during the adsorption process. The capacitance plateau between -0.05 V and -0.45 V is indicative for the steady state adsorption in region III. The desorption process in region IV is illustrated by the increasing capacitance between -0.45 V and -0.69 V.

The same adsorption regions can be seen for AMTD and MMTD in Figure 2, only more pronounced. The pre-adsorption in region I starts at -0.79 V and precedes in the electrochemical adsorption (region II) at -0.59 V. The steady state adsorption is initiated at the switching potential (-0.05 V) and proceeds until -0.59 V. The capacity lapse related to reorganization of organic molecules in solution and electrolyte molecules in solution and on the copper surface determines region IV and is visible until -0.89 V. AMTD and MMTD show identical potential limits for all regions, only the capacitance is shifted to higher values for MMTD. The value of the constant capacity plateau of region III is 6.0 μF cm^{-2} and 8.2 μF cm^{-2} for AMTD and MMTD respectively. A difference in adsorption geometry could be the reason for these diverting capacitance values and the resulting layer thickness.

3.1.2. Potentiodynamic ORP-EIS combined with in-situ SERS

To validate the measurement noise and gather further information on the adsorption process, potentiodynamic odd random phase electrochemical impedance

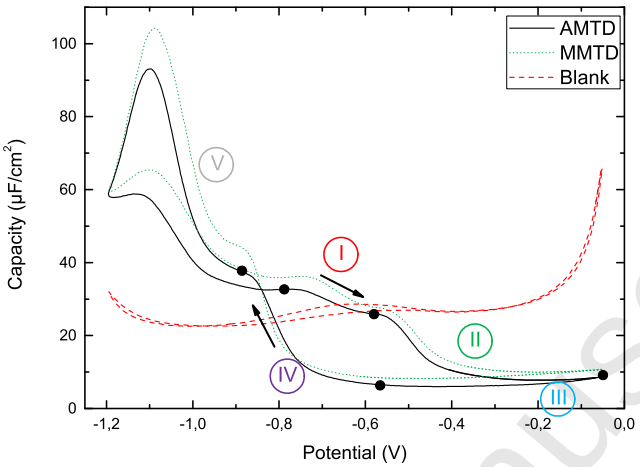

Figure 2: Differential capacitance plots from AC voltammetry of a copper electrode in 0.1 M NaF + 0.005 M AMTD (solid black line) and 0.005 M MMTD (dotted green line). All measurements are obtained after stabilisation through continuous cycling during 24 hours at 2 mV/s.

spectroscopy (PD ORP-EIS) [21, 22] is used in addition to in-situ SERS. This measurement methodology is a continuation of our previous work on MMTD adsorption [11] where a random phase multisine EIS technique was used which provides less statistical information compared to ORP-EIS [25]. Due to the inherent stationary nature of EIS measurements this statistical information is indispensable. Moreover, the total variance will be used as a weighting factor in the EEC modelling procedure. In the previous section a strong adsorption of AMTD, MMTD and triazole was distinguished by AC voltammetry measurements. The detailed study of the adsorption mechanism in this section will therefore be implemented on these molecules.

The experimental data gathered from an ORP-EIS measurement shown in Figure 3 indicate a discrepancy between the total variance (solid blue line) and the measurement noise (green asterisks). On first sight this is an indication of a non-linear contribution originating from the system under study. Since identical distortions appeared to be already present in the input signal that is applied by the potentiostat, they are not caused by the electrochemical system under study. A possible explanation for this phenomenon is the complex construction

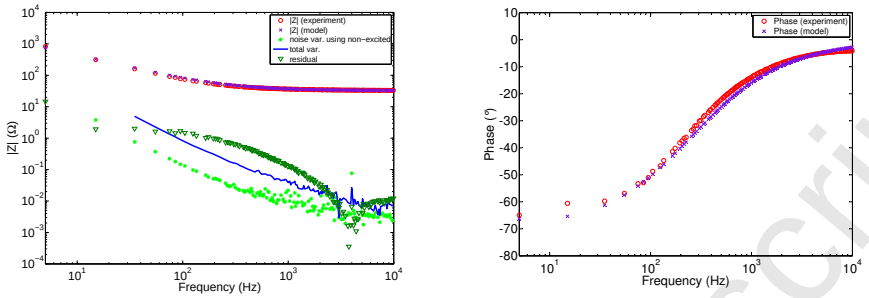

(a) (b)

Figure 3: Comparison between modelled (RRQ model) and experimental impedance with (a) the amplitude and (b) the phase for copper in 0.1M NaF + 0.005M AMTD after 24 hours of immersion with an excitation amplitude of 5 mV, a polarization rate of 2 mV s^{-1} and recorded at -0.75 V in the anodic direction of the linear scan.

of the experimental set-up. In order to perform the PD ORP-EIS measurements simultaneously with the AC Voltammetry, two computers equipped with data acquisition cards, a waveform generator and lock-in-amplifier are all connected to the potentiostat. As a result of this construction, more disturbances from the electrical appliances will be picked up, causing the total variance level of the measurement to differ from the noise level on the non-excited frequencies. Nevertheless, since the total variance level is never above 2.5 % of the magnitude value of the measured impedance, it can be concluded that the obtained PD ORP-EIS data are reliable and thus, can be modelled using an EEC.

The PD ORP-EIS results from this work are fitted to an electrical equivalent circuit (EEC) containing the electrolyte resistance R_E in series with a parallel connection of a resistance R_f (faradaic currents running through the system) and a constant phase element (CPE) Q_T. The CPE is used instead of the overall capacitance C_T to express the surface heterogeneity. Moreover, the power value of the CPE, n_T, can be interpreted as a measure of the layer quality. From that point of view, it is beneficial to use a CPE presentation because it allows to capture this parameter.

To incorporate the disturbances that might be related to the home-built set-

Table 1: Fitting parameters of the potentiodynamic ORP-EIS measurement of AMTD at -0.75 V in the anodic scan using the RRQ model. Results are attained through a total variance weighting.

	fitted value	error (95%)
R_f (Ω)	2.61E+3	3.8E+2
R_e (Ω)	3.25E+1	1.0E-2
Q_T ($s^{n_T}\Omega^{-1}cm^{-2}$)	1.36E-4	4.5E-6
n_T	7.58E-1	4.5E-3

up, the total variance level of the measurements is used as a weighting factor in the modelling of the EEC. Consequently less weight is attributed to data points which are more influenced by these distortions. An example of a modelling result is shown in Figure 3, where the spectrum of AMTD at -0.75 V in the anodic scan is plotted. The fitted parameters and corresponding errors are shown in Table 1.

In Figure 3 the comparison between the experimental and the modelled magnitude (a) is shown beside the overlap of the phase shifts (b). The total variance is implemented as a weighting factor in the EEC modelling to compensate the modest non-linear behaviour in the measured impedance spectrum (deviation between total variance and noise variation using non exited frequencies). The resulting residual curve (green triangles) is less than 1 % of the measured value over the entire frequency range. Since this residual error is small and since no other physically meaningful model can be found, it is feasible to accept the RRQ equivalent electrical circuit to model the PD ORP-EIS data.

The most important parameter retrieved from the PD ORP-EIS measurements concerning the adsorption phenomena is the capacitance. Since a CPE element is used, the fitted value has to be converted towards a pseudo capacitance using the Brug relation [26, 27]. The result of this conversion can be directly compared to the differential capacitance measurements performed ear-

lier in this work. Since the average value of n in the steady state adsorption region is 0.83 the calculated capacitance values from the Brug relation have to be interpreted as rough estimations. However, the relation between the investigated molecules still holds. Pajkossy et al. have shown that the capacitance dispersion observed in the presence of specific adsorption can be assigned either to a slow diffusion or adsorption process or to transformations within the adlayer or the substrate surface rather than inhomogeneous adsorbate layers [28]. Since the link with the adsorption kinetics is maintained in the PD ORP-EIS measurements, this could result in the relatively low values of n.

In Figure 4 the overlay of AC voltammetry and PD ORP-EIS is made for the adsorption of AMTD. The green triangles represent the calculated pseudo capacitance from ORP-EIS samples in the anodic scan and red squares in the cathodic scan. When the corresponding samples are connected, the potentiodynamic ORP-EIS result is qualitatively in good agreement with the differential capacitance curve (solid black line in Figure 4). The four different regions related to the adsorption stages can be seen in identical potential limits. It is clear that the continuous sampling in the differential capacitance measurements provides valuable information on the kinetics of the adsorption process. However, when the capacitance values obtained in both techniques are compared, different values are observed. The capacitance value is overestimated using AC voltammetry. This observation is also made in the blank solution (not shown here). The most plausible reason for the overestimation of the capacitance is the absence of R_f in the model to calculate the differential capacitance curve (at the used frequency of 22 Hz). From the fitting results of the ORP-EIS data, it is clear that the electrochemical adsorption-desorption process of the AMTD molecules causes not only a charge redistribution in the interface region but produces also a faradaic current that runs through the system. Hence, R_f should be incorporated in the model.

In region III (steady state adsorption) on Figure 4, the constant capacitance value is less than half the value that is obtained from the AC voltammetry measurements (6.1 $\mu F\ cm^{-2}$). To calculate the best-fit capacitance value for region

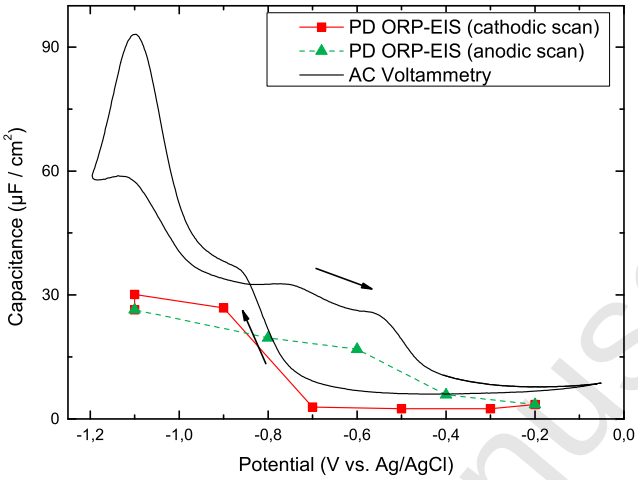

Figure 4: Differential capacitance curve of AMTD from AC voltammetry (solid black line) with overlay of the best fit capacitance values in the anodic (green triangles) and cathodic (red squares) scan direction determined using PD ORP-EIS

III, the weighted mean of the values found at -0.3 V and -0.5 V is calculated and results in 2.5 µF cm^{-2}. The corresponding adsorbate layer thickness to these capacitance values is 0.31 nm and 0.76 nm from AC voltammetry and ORP-EIS respectively ($\epsilon_r = 2.2$). If an identical approach is used for MMTD (Figure not shown here), the capacitance determined by AC voltammetry (8.2 µF cm^{-2}) is adjusted to 2.29 µF cm^{-2}. This results in an adsorbate layer thickness of 0.24 nm (AC voltammetry) and 0.85 nm (ORP-EIS).

To correlate the measured capacitance values to a possible adsorption geometry, quantum chemical calculations can be used. The optimised molecular geometry of AMTD and MMTD indicates four possible adsorption modes shown in Figure 5: (1) N^3- N^4-Cu σ-bonding, (2) N^4-S-Cu σ-bonding, (3) S-Cu π-bonding and (4) S^1-S-Cu σ-bonding. The thickness of one molecular layer (ML) for every orientation is 0.24 nm, 0.33 nm, 0.55 nm and 0.34 nm respectively. The use of ORP-EIS thus seems to indicate the presence of several monolayers of adsorbate molecules rather than one molecular layer adsorbed through the N^4-S-Cu (2) or S^1-S-Cu (4) σ-bonds as AC voltammetry measurements suggest.

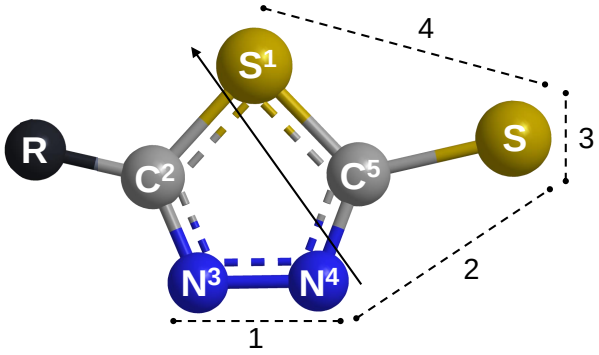

Figure 5: Possible adsorption modes of AMTD (R = NH_2) and MMTD (R = CH_3) on copper. The dashed lines represent the copper surface and the numbers 1 to 4 the possible adsorption modes: (1) N^3- N^4-Cu σ-bonding, (2) N^4-S-Cu σ-bonding, (3) S-Cu π-bonding and (4) S^1-S-Cu σ-bonding. The black arrow shows the direction of the molecular dipole moment.

Since none of the electrochemical measurement techniques, AC voltammetry or ORP-EIS, can provide a direct physical interpretation in-situ SERS is performed. An attempt will be made in this section to reduce the remainder of the hiatuses in the adsorption mechanism using the direct molecular information from SERS. Besides potential, also polarisation rate proved an important parameter in the layer formation of MMTD [11]. Therefore SERS measurements are applied in-situ during a cyclic polarisation. SERS and Raman spectra can differ substantially because adsorbate vibrational frequencies are changed on binding to the SERS substrate. SERS does not enhance all vibrations equally, causing relative Raman band intensities to change. From these differences valuable information can be gathered on the orientation of the adsorbate and its bonding to the surface. Intensity variations can however be caused by the potential dependency of the adsorption process or by orientation effects. The correlation of SERS intensity changes with a change in the surface concentration of adsorbed species is therefore not straightforward. The SERS spectrum for AMTD is given in Figure 6(a), assignment of the vibrational frequencies was proposed by Yang et al. [29] and is used in this work. AMTD shows six peaks in the SERS spectrum over the range of 900 cm^{-1} to 1650 cm^{-1}. The vibrational assignment for the peaks are a C^5-S-H rocking vibration at 1034 cm^{-1}, a C=N-N asymmetric

stretch at 1143 cm^{-1}, an in-plane ring bend at 1326 cm^{-1}, a ring C^5-N^4 stretch at 1390 cm^{-1} and finally a N^4-H rocking vibration at 1499 cm^{-1}. These assignments are an indication that the previously proposed N^4-S-Cu σ-bonding occurs. Consequently the capacitance values for the steady-state adsorption plateau obtained by ORP-EIS suggest an additional molecular layer is adsorbed. Another observation that has been made is the sometimes large frequency shift between the Raman and SERS peaks for AMTD and MMTD in comparison with the small heterocycles. This indicates a stronger adsorbate-surface interaction for AMTD and MMTD, resulting in altered vibrational frequencies.

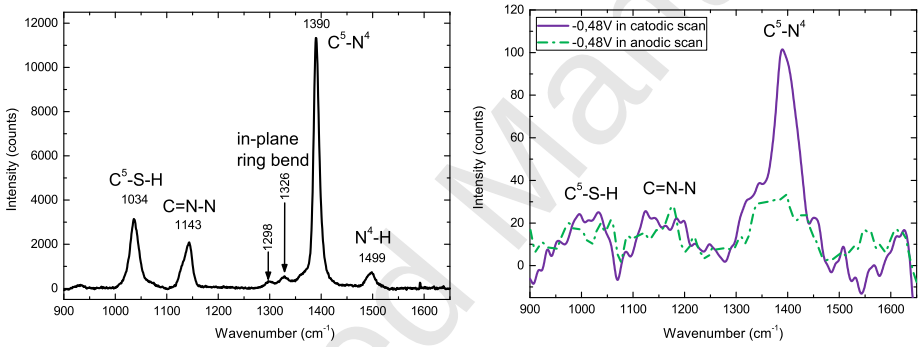

(a) (b)

Figure 6: SERS spectra of 0.1 M NaF + 0.005 M AMTD aqueous solution on a SERS-active copper surface: (a) without potential control and (b) recorded at -0.48 V in the anodic direction (green dashed-dotted line, region II) and at -0.48 V in the cathodic direction (purple solid line, region IV) of the linear scan

The in-situ SERS spectra are recorded during the potential variation on the copper surface. The results are visualized as a 3D-graph with the different potential steps of the cyclic potential scan plotted on the z axis. To compare the SERS results with the PD ORP-EIS results, the spectra are grouped according to the different adsorption regions. By looking at the grey and red SERS curves in Figure 7, it is clear that there is no or little interaction between AMTD and the copper surface in regions V and I (the pre-adsorption region). From -1.02 V to -0.66 V (on the left) and from -0.84 V to -1.16 V (on the right) few to no peaks are visible. Only the peak of the C^5-N^4 stretch at 1390 cm^{-1} sometimes

appears in the SERS spectra. Its low relative intensity confirms that only few AMTD molecules are adsorbed on the copper surface. This is in agreement with the low surface coverage measured with AC voltammetry as well as PD ORP-EIS. When a potential value of -0.30 V is reached in the anodic direction of the linear scan, the measured scattering intensity suddenly increases. The electrochemical adsorption stage (region II) is clearly reached at this potential. At the end of region II, in the steady state adsorption region (region III) and at the beginning of the desorption region (region IV), SERS spectra are recorded with a maximum scattering intensity obtained at a potential of 0.07 V. The only difference with the AC voltammetry results (Figure 2) is that the desorption process seems to start at a potential of -0.48V compared to -0.60V.

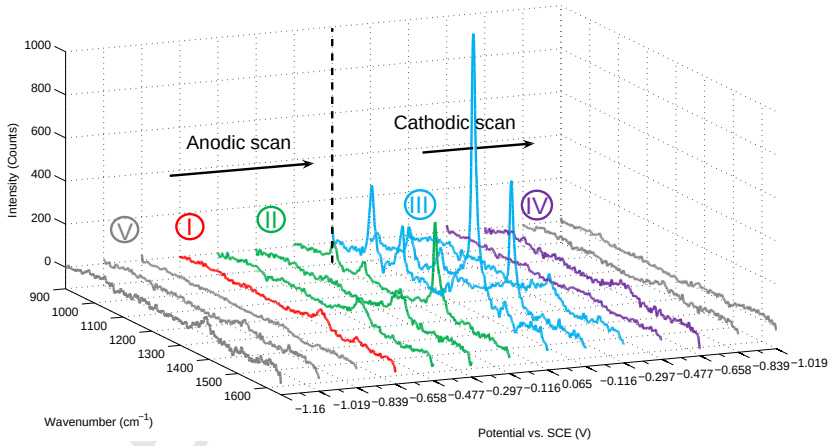

Figure 7: Potential dependant SERS spectrum of AMTD

Another important observation is the different SERS response recorded at -0.48 V in the anodic scan and at the same potential in the cathodic scan. This is illustrated in Figure 6(b). The different capacitive behaviour that was observed in the previous section (Figure 4) for the two potential points, is now confirmed by their different SERS response. It can be concluded that more AMTD molecules are adsorbed at -0.48 V in region III than at the beginning of region II. Hence, it indicates that the SERS measurements under potential

scan reflect the kinetics of the organic layer deposition.

The fitted capacitance values from PD ORP-EIS of triazole in overlay with the differential capacitance curve is shown in Figure 8. As with AMTD an overestimation of the capacitance values from AC voltammetry is visible in the anodic as well as the cathodic scan direction, however the course of the curves from both techniques is similar. Due to the smaller number of samples obtained during PD ORP-EIS the features of the anodic and cathodic scans are less pronounced compared to the AC voltammetry curve. The position of the capacitance plateau in the AC voltammetry curve (-0.15 V to -0.45 V, solid black line) is 8.8 µF and amounts to 0.21 nm (ϵ_r=2.2). The samples at -0.2 V and -0.35 V of the cathodic scan (red squares) in the steady state adsorption region give an average capacitance of 4.1 µF which relates to a layer thickness of 0.46 nm. Since the thickness of one adsorbate ML of triazole (N^1- N^2-Cu σ-bonding) is 0.22 nm, the ORP-EIS results rebut the presence of only a single ML. A plausible explanation would the adsorption of additional molecular layers, comparable to the AMTD adsorption.

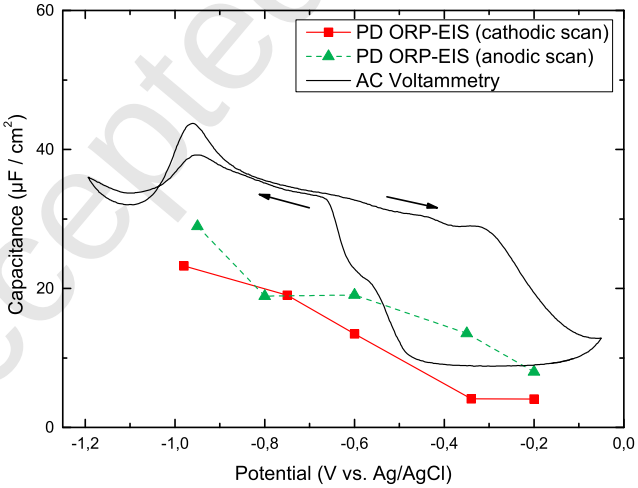

Figure 8: Differential capacitance curve of triazole from AC voltammetry (solid black line) with overlay of the best fit capacitance values in the anodic (green triangles) and cathodic (red squares) scan direction determined using potentiodynamic ORP-EIS

The in-situ SERS graph of triazole (Figure 9) shows a comparable evolution

as with AMTD and MMTD. In region V there still seems to be adsorption present, this can be linked to the local decrease in capacitance values in the AC voltammetry curve (Figure 1). In region I which starts at -0.61 V the intensity of the peaks is low. There is little adsorption during this reorganization process. Starting at -0.25 V an increase in peak intensities occurs. This potential determines the electrochemical adsorption region. The potential range, with an increasing amount of adsorbed molecules, goes through the positive end of the potential scan and amounts to a maximum intensity value at -0.43 V. This maximum is located in the steady state adsorption region. After this maximum the electrochemical desorption slowly sets in and continues through the more negative end of the potential range to finally amount in low intensity values at -0.61 V.

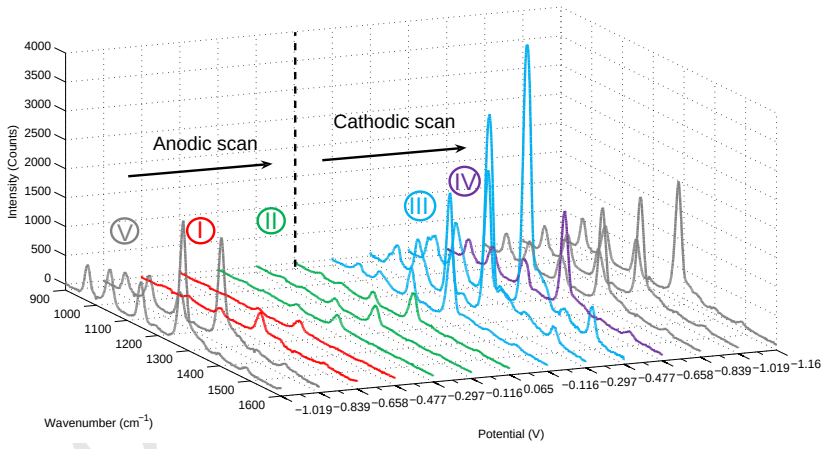

Figure 9: Potential dependant SERS spectrum of triazole

4. Conclusions

Comparison of the differential capacitance graphs of triazole and imidazole, clearly indicates that only a small change in substituted atoms in the ring structure (deletion of one nitrogen atom) greatly affects the adsorption pro-

cess. Consequently the prior stated conclusion that adjacent nitrogen molecules cause good inhibiting properties can be directly related to the adsorption mechanism of these molecules. Pyrazine and pyridazine display only minor to none adsorption and desorption behaviour.

The application of PD ORP-EIS proved to be favourable over the differential capacitance data, possibly due to the frequency dispersion of the investigated system. By comparing the PD ORP-EIS data with the results obtained by means of classical AC voltammetry, it is concluded that the latter are only qualitatively correct and cannot be used to calculate the correct layer thickness. Moreover, the AC voltammetry results provide no error estimates on the obtained results.

The combination of experimental techniques (electrochemical and spectroscopic) allowed the elucidation of the adsorption mechanism of AMTD and MMTD. The adsorption geometry of both molecules on a copper surface is determined by the N^4-S-Cu σ-bond while the applied polarisation rates induced the deposition of more than one molecular layer. The adjacent nitrogen atoms in triazole define the adsorption centre on copper (N^1- N^2-Cu σ-bonding). As with AMTD and MMTD, the 2 mV s^{-1} scan rate induces multiple adsorbed ML of triazole on copper.

References

[1] Y. Arima, H. Iwata, Biomaterials 28 (2007) 3074.

[2] I. Van De Keere, R. Willaert, A. Hubin, J. Vereecken, Langmuir 24 (2008) 1844.

[3] L. Wang, M. Yoon, A. Facchetti, T. Marks, Advanced Materials 19 (2007) 3252.

[4] O. Blajiev, A. Hubin, Electrochimica Acta 49 (2004) 2761–2770.

[5] C. Brosseau, J. Leitch, X. Bin, M. Chen, S. Roscoe, J. Lipkowski, Langmuir 22 (2008) 13058.

[6] D. Cahen, A. Kahn, E. Umbach, Materials Today 7 (2005) 32.

[7] B. Trachli, M. Keddam, H. Takenouti, A. Srhiri, Corrosion Science 44 (2002) 997–1008.

[8] K. Khaled, M. a. Amin, Corrosion Science 51 (2009) 2098–2106.

[9] A. L. Eckermann, D. J. Feld, J. a. Shaw, T. J. Meade, Coordination chemistry reviews 254 (2010) 1769–1802.

[10] O. Blajiev, T. Breugelmans, R. Pintelon, a. Hubin, Electrochimica Acta 51 (2006) 1403–1412.

[11] O. L. Blajiev, T. Breugelmans, R. Pintelon, H. Terryn, A. Hubin, Electrochimica Acta 53 (2008) 7451–7459.

[12] D. Gonnissen, W. Langenaeker, A. Hubin, P. Geerlings, Journal of Raman Spectroscopy 29 (1998) 1031.

[13] O. Blajiev, H. Terryn, A. Hubin, L. Soukupova, P. Geerlings, Journal of Raman Spectroscopy 37 (2006) 777.

[14] M. Weaver, J. Hupp, F. Barz, J. Gordon, M. Philpott, Journal of Electroanalytical Chemistry 160 (1984) 321.

[15] L. Stolberg, J. Lipkowski, D. Irish, Journal of Electroanalytical Chemistry 300 (1991) 563.

[16] A. J. Shen, J. Pemberton, Journal of Electroanalytical Chemistry 479 (1999) 21.

[17] R. Aroca, R. E. Clavijo, M. D. Halls, H. B. Schlege, Journal of Physical Chemistry A 104 (2000) 9500.

[18] B. Pettinger, A. Fiedrich, U. Tiedemann, Journal of Electroanalytical Chemistry 280 (1990) 49.

[19] A. Otto, I. Mrozek, H. Grabhorn, W. Akemann, Journal of Physics-Condensed Matter 4 (1992) 1143.

[20] T. Breugelmans, J. Lataire, T. Muselle, E. Tourwé, R. Pintelon, A. Hubin, Electrochimica Acta 76 (2012) 375–382.

[21] E. Van Gheem, R. Pintelon, J. Vereecken, J. Schoukens, A. Hubin, P. Verboven, O. Blajiev, Electrochimica Acta 49 (2004) 4753–4762.

[22] E. Van Gheem, R. Pintelon, A. Hubin, J. Schoukens, P. Verboven, O. Blajiev, J. Vereecken, Electrochimica Acta 51 (2006) 1443–1452.

[23] A. Kudelski, J. Bukowska, M. Janik-Czachor, W. Grochala, A. Szummer, M. Dolata, Vibrational Spectroscopy 16 (1998) 21–29.

[24] J. Bockris, A. K. N. Reddy, M. Gamboa-Aldeco, Modern Electrochemistry Volume 2A, Kluwer academic publishers, New York, 2000.

[25] T. Breugelmans, E. Tourwé, J.-B. Jorcin, A. A. Pampliega, B. Geboes, H. Terryn, A. Hubin, A. Alvarez-Pampliega, B. Geboes, H. Terryn, A. Hubin, Progress in organic coatings 69 (2010) 215–218.

[26] G. Brug, A. Van den Eeden, M. Sluyters-Rehbach, J. Sluyters, Journal of Electroanalytical Chemistry 176 (1984) 275–295.

[27] J.-B. Jorcin, M. E. Orazem, N. Pébère, B. Tribollet, Electrochimica Acta 51 (2006) 1473–1479.

[28] T. Pajkossy, T. Wandlowski, D. Kolb, Journal of Electroanalytical Chemistry 414 (1996) 209–220.

[29] H. Yang, W. Song, J. Ji, X. Zhu, Y. Sun, R. Yang, Z. Zhang, Applied Surface Science 255 (2008) 2994–2999.

Acknowledgements

The authors would like to thank Dr. Ian Burgess for providing the LabView programs for cyclic voltammetry and differential capacitance measurements.